

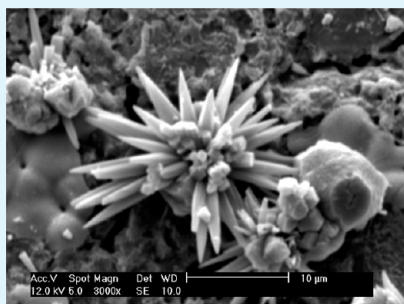
Effect of Nanospinel Additions on the Sintering of Magnesia–Zirconia Ceramic Composites

R. M. Khattab,^{*,†} M. M. S. Wahsh,[†] N. M. Khalil,^{‡,†} F. Gouraud,[§] M. Huger,[§] and T. Chotard[§]

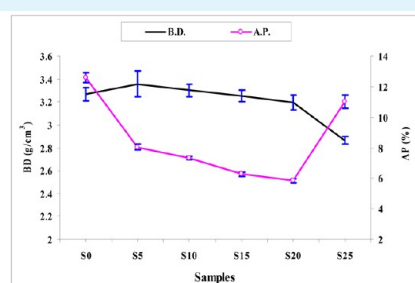
[†]Refractories, Ceramics and Building Materials Department, National Research Centre, 12311 Cairo, Egypt

[‡]Department of Chemistry, Faculty of Sciences and Arts, Khulais, King Abdulaziz University, Jeddah 21589, Saudi Arabia

[§]Laboratoire de Science des Procédés Céramiques et Traitements de Surface, SPCTS UMR 7315 CNRS, European Ceramic Centre (CEC), 12 Rue Atlantis, 87068 Limoges, France



SEM micrograph for the sintered samples S10



Bulk density and apparent porosity of the sintered samples S0–S25

ABSTRACT: Nanocrystalline magnesium aluminate (MA) spinel powder produced through a coprecipitation method and calcined at 900°C for 1 h was added to magnesia–zirconia composite in the range of 0–25 mass % and sintered at 1600°C for 2 h. Scanning electron microscope (SEM) and X-ray diffraction (XRD) techniques were used for studying the microstructure and the phase composition of the sintered composites. Bulk density, apparent porosity, volume shrinkage, and Young's modulus of the sintered composites were also investigated. The results revealed that the nanospinel addition up to 20 mass % increases the sintering ability and Young's modulus of the composite bodies. Microstructure showed that the presence of nanospinel and zirconia in the triple point between magnesia grains closed the gaps in the ceramic matrix and enhanced the compactness of the composites.

KEYWORDS: ceramics, composites, sintering, microstructure, Young's modulus

INTRODUCTION

Composite materials are considered as the matter of interest of several research works conducted during the last three decades because of their outstanding refractory, physical, and mechanical properties which make them suitable for high temperature and engineering applications.¹

In the past decade, a significant amount of work has been done to further enhancement of the strength and fracture toughness of composite materials by incorporating nanosize dispersions within the matrix grains.¹ Among the studied nanocomposites, nanospinel bearing materials have been recognized as one of the most effective ceramic material due to their excellent properties.²

Magnesia ceramics have good resistance to basic slags and clinkers to be used in cement rotary kilns and steel ladles. However, magnesia has some shortcomings, such as high thermal conductivity, poor spalling and penetration resistance. The basic properties of MgO were modified by mixing it with other metallic ion or metal oxides like ZrO₂ to produce ceramic materials having superior properties.^{3–5} In order to avoid the shortcomings mentioned above, oxides such as SiO₂, Al₂O₃,

Cr₂O₃, TiO₂, ZrO₂, and WO₃ were added into ceramics.^{6,7} These oxides may react with MgO to form a second phase to improve sintering of MgO.

Zirconia (ZrO₂) is a very important engineering material because of its unique physicochemical and refractory characteristics such as high refractoriness, corrosion and wear resistance, low coefficient of friction, high fracture toughness and hardness, ionic conduction, low thermal conductivity at high temperature, resistance to thermal shock,⁸ and catalytic properties.^{10,11} Despite these unique characteristics, ZrO₂ has a serious drawback for use as an engineering material because it undergoes phase transformations from the thermodynamically stable monoclinic with a change of volume during a high temperature cycle that are substantial enough to make the pure material unsuitable for applications requiring an intact solid structure: *c* → *t* approximately 2.31%; *t* → *m* approximately 4.5%. So, zirconia stabilized by metal oxide like MgO, CaO, or

Received: November 25, 2013

Accepted: February 6, 2014

Published: February 6, 2014

Y_2O_3 has shown an outstanding structural stability and increases the high oxygen mobility and oxygen storage capacity (OSC) of the ceramic for a majority of the current applications.^{9,10}

Magnesium aluminate spinel ($MgAl_2O_4$) is characterized with a high melting point (2135 °C), low reversible thermal expansion, and high thermal shock resistance as well as excellent erosion and corrosion by slag and molten metals. The combination of these properties in spinel ceramics enables their use at high temperature and engineering applications.^{11–14} One of the drawbacks of spinel ceramic is its insufficient mechanical properties which limit its practical and potential uses in other fields. Intense research has been intended to improve the mechanical strength of $MgAl_2O_4$ through combination with other ceramic materials, e.g., zirconia and magnesia, that are expected to improve its thermomechanical properties. The optimum characteristics of zirconia–magnesia–spinel composite ceramics should be achieved through controlling the contents of their constituents.^{15–19}

This work aims at studying the effect of nanospinel powder additions on the sintering of a magnesia–25 mass % zirconia composite.

2. EXPERIMENTAL SECTION

2.1. Starting Materials and Methods. The materials used were reagent grade chemicals consisting of aluminum chloride hexahydrate ($AlCl_3 \cdot 6H_2O$; Merck Schuchardt OHG, Hohenbrunn, Germany) and magnesium chloride hexahydrate ($MgCl_2 \cdot 6H_2O$; S.D. Fine Chem. Ltd., India) for preparing nanospinel powder.²⁰ Highly pure magnesia (VWR International Ltd., England, with particle size $\leq 20 \mu m$), and pure zirconia ($ZrO_2 \sim 99$ mass %, Sigma–Aldrich with particle size of $5 \mu m$) were also used to prepare magnesia–zirconia composite samples.

2.2. Synthesis of Nanospinel Powder. A nanospinel powder with average crystalline size ~ 33 nm was prepared via a coprecipitation method and then calcined at 900 °C for 1 h, as described in a previous work.²⁰

2.3. Preparation of Magnesia–Zirconia–Nanospinel Composite. Different mixes of magnesia–zirconia–nanospinel composite were prepared by adding 0–25 mass % nanospinel at the expense of zirconia content as seen in Table 1. Each mix was carefully weighed

Table 1. Sample Compositions of Magnesia–Zirconia–Nanospinel Composite

sample	magnesia	zirconia	nanospinel
S0	75	25	0
S5	75	20	5
S10	75	15	10
S15	75	10	15
S20	75	5	20
S25	75	0	25

and mixed by a mechanical ball mill machine (Retsch PM 100) for 2 h using zirconia balls as the milling media and pressed by uniaxial pressing at 100 MPa. Finally, the prepared samples were sintered at 1600 °C for 2 h in air.

2.4. Characterization. Phase analysis was investigated through X-ray diffraction (XRD instrumental D8 ADVANCE, Bruker, Germany; monochromatic beam with $K\alpha_1$ Cu, Bragg Brentano geometry Θ . 2Θ and linear detector LYNX EYE 174 channels 2 s/channel, total time = 348 s). The sintering parameters in terms of bulk density and apparent porosity of the fired compacts were determined after firing at 1600 °C for 2 h, according to ASTM-C20 method. The volume shrinkage of the bodies was determined by measuring the dimensional changes before and after the sintering process. The microstructure was examined

using scanning electron microscope (Philips XL 30) of gold coated fractured sample. For sintered samples, Young's modulus was measured using the reflection method.²⁰ Indeed, the dense character of samples allowed the propagated signal to be less disturbed by microstructure singularities then round trip and higher working frequency (10 MHz) permit to produce reliable data on velocities. For this case, the transit time, τ , representing the round trip time through the thickness of the sample d is measured and is related to wave velocity, V_L , as follows:

$$V_L = \frac{2d}{\tau}$$

3. RESULT AND DISCUSSION

3.1. XRD of the Sintered Composites. X-ray diffraction patterns of samples S0–S25 sintered at 1600 °C for 2 h are given in Figure 1. As can be seen from this figure, sample S0 shows only the crystalline phases of periclase and cubic zirconia. This is due to the fact that according to the phase diagram of binary MgO – ZrO_2 system, there are no binary compounds in the MgO – ZrO_2 system,²¹ the solubility of MgO in different polymorphs of ZrO_2 varies with temperature. The solubility of MgO in monoclinic ZrO_2 is negligible up to tetragonal transformation; it increases slowly with temperature but still less than 1% at 1300 °C. A cubic solid solution becomes stable at 1400 °C with an eutectoid at 13 mol % MgO . Homogeneous solid solution then exists at this composition above 1400 °C. Analysis of the XRD patterns S5, S10, S15, and S20 reveals that the detected phase are the periclase, cubic zirconia, and spinel; except for sample S25 in which only periclase and spinel were detected. With increase of spinel additions, the intensity of $MgAl_2O_4$ peaks increases and cubic ZrO_2 peaks decreases from S5 to S20.

3.2. Densification Parameter. As shown in Figure 2, apparent porosity values decrease significantly with the addition of nanospinel, which reach to lower value in sample S20 (5.85%) compared to magnesia–zirconia (12.59%) and magnesia–spinel (11.02%) samples. Further, the open porosity values of magnesia–spinel containing a high amount of zirconia composite as such as S5 (8.05 %) are higher than those of magnesia–spinel samples containing a high amount of nanospinel. On the contrary, the density values rise continuously with increasing amounts of zirconia that reach a maximum in the S5 (3.36 g/cm³) sample. The gradual increase in the bulk density of the sintered composites with zirconia content is due to the relatively higher theoretical density of zirconia (5.68 g/cm³) than $MgAl_2O_4$ spinel (3.57 g/m³) and magnesia (3.58 g/cm³). Little decrease in apparent porosity with incorporation of nanospinel may be related to the presence of the nanospinel phase which enhances the compactness between magnesia and zirconia grains by filling up the intergranular voids.²² Also, the formation of cubic zirconia is responsible for generating spherical voids by releasing high pressure oxygen which increases the apparent porosity with a high amount of zirconia content.²³ With the addition of a small amount of zirconia (5 mass %), an improvement was observed in the sinterability of magnesia/ $MgAl_2O_4$ spinel ceramic. This is due to that Zr^{4+} goes into the MgO lattice and formed magnesium ion vacancies which accelerated the diffusion of oxygen to generate dense product. Another reason for the improvement of the sinterability is the existence of the ZrO_2 at the grain boundary which controls the grain growth of magnesia by promoting the diffusion of the oxygen between the boundary.^{11,24,25}

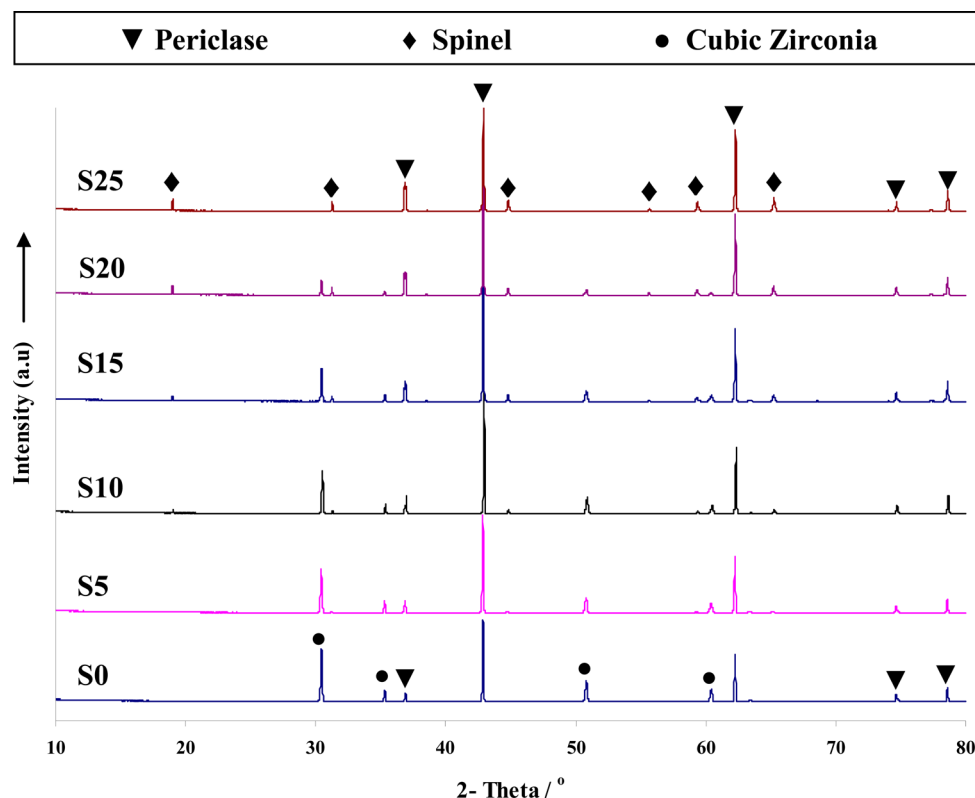


Figure 1. XRD of the sintered samples S0–S25 fired at 1600 °C.

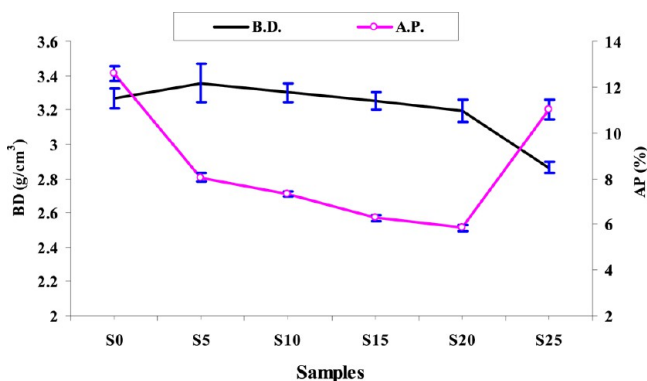


Figure 2. Bulk density and apparent porosity of the sintered samples S0–S25 fired at 1600 °C.

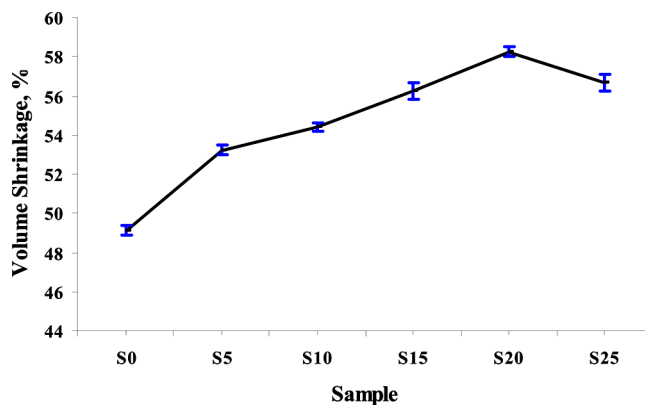


Figure 3. Volume shrinkage of the sintered samples S0–S25 fired at 1600 °C.

3.3. Volume Shrinkage. Figure 3 shows the volume shrinkage of the magnesia–zirconia–nanospinel composite with the different nanospinel contents. The increase of volume shrinkage with increasing nanospinel content was observed. The volume shrinkage increases from 49% to 58% with increasing nanospinel content. This also proved the above established fact that the densification process will begin at a relatively lower temperature for ceramics made from nanopowders where faster pore elimination and a sluggish grain growth occur.^{26,19}

3.4. Young's Modulus. The modulus of elasticity E (Young's modulus) values of magnesia–zirconia–spinel in general increase with increasing nanospinel content up to 20 mass % and, then, decrease with further additions of nanospinel, as shown in Figure 4. With incorporation of 20 mass % of nanospinel, the modulus of elasticity values have displayed a marked increase (48.5 GPa) compared to

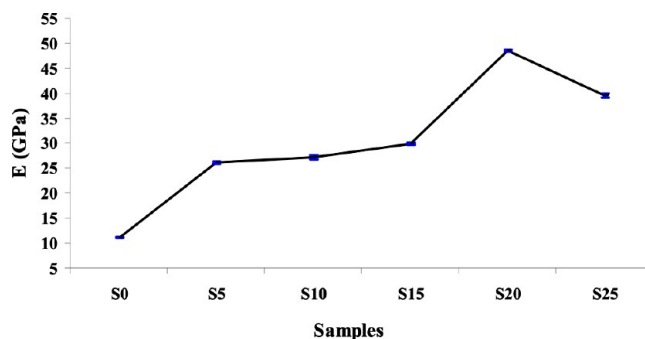


Figure 4. Young's modulus of the sintered samples S0–S25 fired at 1600 °C.

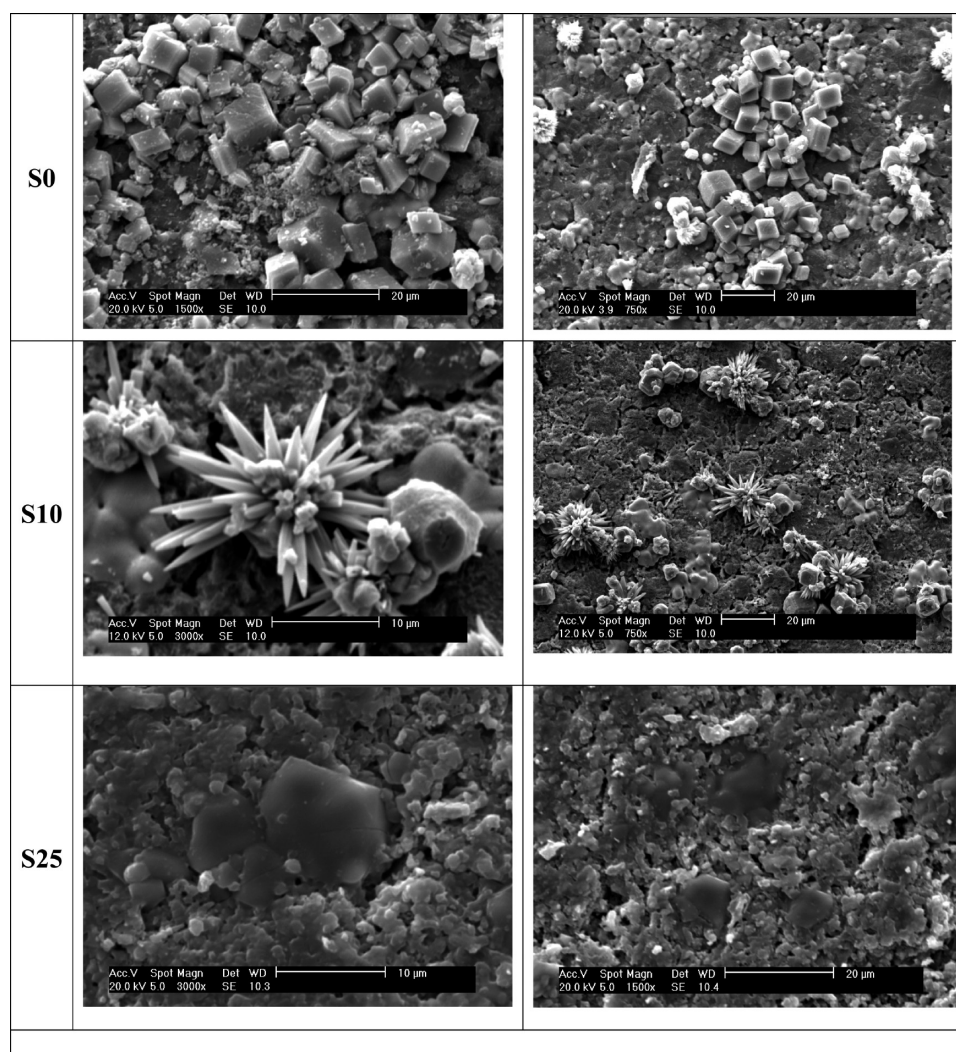


Figure 5. SEM micrograph for the sintered samples S0, S10, and S25 fired at 1600 °C.

magnesia–spinel and magnesia–zirconia materials. This is due to the difference between the thermal expansion coefficients (α) of MgO, spinel, and zirconia¹⁵ (α MgO = $13.6 \times 10^{-6} \text{ }^\circ\text{C}^{-1}$, α spinel = $8.4 \times 10^{-6} \text{ }^\circ\text{C}^{-1}$, and α cubic zirconia = $10.5 \times 10^{-6} \text{ }^\circ\text{C}^{-1}$) which creates significant tensile stresses around additives. Such stresses cause the formation of interlinked microcracks that are propagated for a short distance then arrested when coming across spinel (large particle), i.e., large grains act as obstacles on a plane where the crack propagated.^{27,28}

3.5. Microstructural Evaluation of Sintered Compacts.

The SEM micrograph (Figure 5) for S0, S10, and S25 samples showed that the periclase matrix appeared in polyhedral grains with sizes less than 1–4 μm . The cubic zirconia found in three different shapes first appeared in small spherical white shape with size of 0.5–2 μm then grow to flower shape and finally convert to cubic form with diameters of 5–8 μm . They were present not only on grain boundaries but also inside the large grains as seen in S0 and S10 samples. Nanospinel additions enhanced the microstructural features of magnesia–zirconia samples, which fills the intergranular spaces and tend to agglomerate between the periclase grains in platelet-like shaped with size 5–20 μm . The nanospinel agglomeration is related to many nanospinel–nanospinel grain boundary connections

which reduced the grain growth of MgO grains through grain boundary pinning.

4. CONCLUSION

Addition of nanospinel powder up to 25 mass % exert on the properties of magnesia–zirconia composite after sintering at 1600 °C for 2 h. Adding nanospinel enhanced the sintering to occur in the lower temperature because of the difference of surface area energy between the matrix and the nanospinel particles. The results of young modulus showed that the marked improvement in elastic modulus (48.5 GPa) can be obtained in those samples with 20 mass % nanospinel. The sintering parameters of these samples were $\sim 3.2 \text{ g/cm}^3$ (BD) and $\sim 5.8\%$ (AP). The spinel particles are homogeneously dispersed at the grain junctions of the periclase matrix and suppress grain growth by grain boundary pinning and thereby lower the flow stress. Therefore, longer service life is predicted for magnesia–zirconia–spinel composite at high temperatures in industrial use.

■ AUTHOR INFORMATION

Corresponding Author

*E-mail: rihamkhattab78@yahoo.com. Fax: +20233370931.

Notes

The authors declare no competing financial interest.

REFERENCES

- (1) Joon, H. L.; Ickchan, K.; Dustin, M. H.; Dongtao, J.; Amiya, K. M.; Xinghang, Z.; Haiyan, W. Grain and grain boundary activities observed in alumina–zirconia–magnesia spinel nanocomposites by in situ nanoindentation using transmission electron microscopy. *Acta Mater.* **2010**, *58*, 4891–4899.
- (2) Rashmi, R. D. Effect of micron and nano MgAl_2O_4 spinel addition on the properties of magnesia-carbon refractories. M. Sc. Thesis, Department of Ceramic Engineering National Institute of Technology, Rourkela, 2010.
- (3) Peng, C.; Li, N.; Han, B. Effect of zircon on sintering, composition and microstructure of magnesia powders. *Sci. Sintering* **2009**, *41*, 11–17.
- (4) Aramendía, M. A.; Boráu, V.; Jiménez, I. C.; Marinas, A.; MaSrinias, J.M.; Navío, J. A.; Ruiz, J.R.; Urbano, F. J. Synthesis and textural-structural characterization of magnesia, magnesia–titania and magnesia–zirconia catalysts. *Colloids Surf. A: Physicochem. Eng.* **2004**, *234*, 17–25.
- (5) Han, B.; Li, Y.; Guo, C.; Li, N.F. Sintering of MgO-based refractories with added WO_3 . *Ceram. Int.* **2007**, *33*, 1563–1567.
- (6) Martinac, V.; Labor, M.; Petric, N. Effect of TiO_2 , SiO_2 and Al_2O_3 on properties of sintered magnesium oxide from seawater. *Mater. Chem. Phys.* **1996**, *46*, 23–30.
- (7) Nishida, A.; Fukuda, S.; Kohtoku, Y.; Terai, K. Grain size effect on mechanical strength of MgO– ZrO_2 composite ceramics. *J. Ceram. Soc. Jpn.* **1992**, *100*, 191–195.
- (8) Ray, J.C.; Park, D.W.; Ahn, W.S. Chemical synthesis of stabilized nanocrystalline zirconia powders. *J. Ind. Eng. Chem.* **2006**, *12*, 142–148.
- (9) Kelly, J.R.; Denry, I. Stabilized zirconia as a structural ceramic: An overview. *Dental Mater.* **2008**, *24*, 289–298.
- (10) Aytumur, A.; Uslu, I.; Kocyiğit, S.; Özcan, F. Magnesia stabilized zirconia doped with boron, ceria and gadolinia. *Ceram. Int.* **2012**, *38*, 3851–3856.
- (11) Suzuki, T.; Itatani, K.; Aizawa, M.; Scott, Howell F.; Kishioka, A. Sinterability of spinel (MgAl_2O_4)-zirconia composite powder prepared by double nozzle ultrasonic spray pyrolysis. *J. Eur. Ceram. Soc.* **1996**, *16*, 1171–1178.
- (12) Khalil, N. M. A review of recent developments in magnesia-spinel refractory composites. *Interceram* **2009**, *58*, 20–25.
- (13) Khalil, N.M. Preparation and characterization of mullite/zirconia and spinel/zirconia composites. *Refractories Eng.* **2007**, *3*, 32–34.
- (14) Khalil, N. M.; Hassan, M. B.; Ewees, E. M.; Saleh, F. A. Preparation and characterization of nanospinel powder via coprecipitation and sol-gel techniques. *Main Group Chem.* **2013**, *12*, 331–347.
- (15) Ceylantekin, R.; Aksel, C. Improvements on corrosion behaviours of mgo–spinel composite refractories by addition of ZrSiO_4 . *J. Eur. Ceram. Soc.* **2012**, *32*, 727–736.
- (16) Maschio, R.D.; Fabbri, B.; Fiori, C. Industrial Applications of Refractories Containing Magnesium Aluminate Spinel. *Ind. Ceram* **1988**, *8*, 121–26.
- (17) Fujita, M.; Yoshimatsu, H.; Osaka, A.; Miura, Y. Preparation and properties of ZrO_2 -dispersed MgO– Al_2O_3 ceramic. *J. Ceram. Soc. Jpn.* **1995**, *103*, 81–84.
- (18) Khalil, N. M. Recent developments in magnesia-spinel refractory composites. *Interceram, Paper Review* **2008**, *57*, 417–422.
- (19) Khalil, N.M.; Wahsh, M.M.S.; Ewais, E.M.M.; Hassan, M.B.; Mehrez, S.M. Improvement of Mullite and Magnesia-Based Refractory Castables Through Addition of Nano-Spinel Powder. *Int. J. Appl. Ceram. Technol.* **2013**, *10*, 655–670.
- (20) Wahsh, M.M.S.; Khattab, R.M.; Khalil, N.M.; Gouraud, F.; Huger, M.; Chotard, T. Fabrication and technological properties of nanoporous spinel/forsterite/zirconia ceramic composites. *Mater. Des.* **2014**, *53*, 561–567.
- (21) Coughanour, W.; Roth, R.S.; Marzullo, S.; Sennett, F.E. Solid-State Reactions and Dielectric Properties in the Systems Magnesia-Zirconia-Titania and Lime-Zirconia–Titania. *J. Res. Natl. Bur. Stand.* **1955**, *54*, 191–199.
- (22) Ghosh, A.; Sarkar, Ritwik; Mukherjee, B.; Das, S.K. Effect of spinel content on the properties of magnesia–spinel composite refractory. *J. Eur. Ceram. Soc.* **2004**, *24*, 2079–2085.
- (23) Ebadzadeh, T. Reaction sintering of multicomponent mixtures for producing ceramics containing zirconia. *J. Eur. Ceram. Soc.* **2000**, *20*, 725–729.
- (24) Yamaguchi, G.; Nakano, M.; Saito, K. Role of oxygen in spinel formation from MgO and Al_2O_3 . *Yogyo-Kyokai-Shi* **1971**, *79*, 92–96.
- (25) Ganesh, I.; Sundararajan, G.; Olhero, S.M.; Ferreira, J.M.F. Influence of chemical composition on sintering ability of ZTA ceramics consolidated from freeze dried granules. *Ceram. Int.* **2011**, *37*, 835–841.
- (26) Zawrah, M.F.; Aly, M.H. In situ formation of Al_2O_3 –SiC–mullite from Al-matrix composites. *Ceram. Int.* **2006**, *32*, 21–28.
- (27) Sahin, B.; Aksel, C. Developments on the mechanical properties of MgO– MgAl_2O_4 composite refractories by ZrSiO_4 –3 mol% Y_2O_3 addition. *J. Eur. Ceram. Soc.* **2012**, *32*, 49–57.
- (28) Ganesh, I.; Ferreira, J.M.F. Synthesis and characterization of MgAl_2O_4 – ZrO_2 composites. *Ceram. Int.* **2009**, *35*, 259–264.